Trees, Forests and People 22 (2025) 101053

Contents lists available at ScienceDirect

Trees, Forests and People

journal homepage: www.sciencedirect.com/journal/trees-forests-and-people

Comparative analysis of productivity, transpiration and water use efficiency in three *Eucalyptus* species with different drought tolerance levels

Amanda de Castro Segtowich [a,*], Cassio Rafael Costa dos Santos [b], Maria Leidiane Reis Barreto [c], Nataly Foronda Ortega [c], Felipe Tavares Lima [c], Patrícia Andressa Ávila Franco de Carvalho [c], Juan Sinforiano Delgado Rojas [d], Alexandre de Vicente Ferraz [e], José Leonardo de Moraes Gonçalves [c]

[a] Southern Swedish Forest Research Centre, Swedish University of Agricultural Sciences, Alnarp, Sweden
[b] Federal Rural University of Amazonia (UFRA), Capitão Poço Campus, Capitão Poço, Pará, Brazil
[c] Department of Forest Sciences, ESALQ, University of São Paulo (USP), Piracicaba, São Paulo, Brazil
[d] Agro Ambiência Serv. Agrícolas LTDA, AASA, Piracicaba, São Paulo, Brazil
[e] Institute of Forest Research and Study (IPEF), Piracicaba, São Paulo, Brazil

ARTICLE INFO

Keywords:
Silviculture
Forest hydrology
Ecophysiology
Sap flow
Soil moisture

ABSTRACT

The increasing concern about water usage by highly productive crops, such as those from the *Eucalyptus* genus, coupled with the quest for greater water use efficiency, has intensified due to the expansion of forest plantations into marginal areas in Brazil with lower water availability—a trend likely to be exacerbated by climate change. Understanding the morphological characteristics and key ecophysiological processes that regulate tree growth and water use is crucial for selecting and enhancing drought-tolerant species. This study aimed to assess the growth and productivity of *Eucalyptus grandis* (low drought tolerance), *Eucalyptus urophylla* (moderate drought tolerance), and *Eucalyptus camaldulensis* (high drought tolerance) and their relationship with transpiration and water use efficiency (WUE). We established experimental plots with these three species in Southeastern Brazil. Each species was planted in plots of 380 trees, spaced at 3 m x 3 m. A measurable area of 36 trees per species was used for non-destructive assessments, while the remaining rows were allocated for destructive sampling. We measured growth, above-ground biomass, transpiration, leaf area index (LAI), leaf water potential, effective precipitation, soil moisture, and calculated WUE. *E. grandis* and *E. camaldulensis* transpired more than *E. urophylla* during the assessment. *E. grandis* and *E. urophylla* presented the highest stand WUE for stem wood biomass production throughout the study period (0.94 and 0.63 kg mm^{-1}, respectively). In contrast, *E. camaldulensis* presented the lowest WUE (0.19 kg mm^{-1}). This study underscores the potential role of *E. urophylla* in achieving high productivity with relatively lower water consumption.

1. Introduction

Climate change is increasingly influencing political, economic, environmental, and social decision-making processes worldwide. In Brazil, rising air temperatures and decreasing precipitation rates have been documented across the country (Dubreuil et al., 2019), with projections suggesting more critical scenarios, including more frequent and intense extreme weather events (Avila-Diaz et al., 2020). Simultaneously, Brazil remains one of the world's largest producers of *Eucalyptus*. Growing concerns regarding water consumption by *Eucalyptus* crops and the pursuit of greater water use efficiency have become particularly relevant given the expansion of plantations into marginal areas with lower water availability (Lima et al., 2012; Florêncio et al., 2022). Such changes directly affect the sustainability of forest-based production systems, especially those dependent on large-scale monocultures, such as Eucalyptus.

Tropical forest plantations using *Eucalyptus* genetic materials often use water in similar quantities of available freshwater in local

* Corresponding author.
E-mail addresses: amanda.segtowich@slu.se (A.C. Segtowich), cassio.santos@ufra.edu.br (C.R.C. Santos), marialeidiane@usp.br (M.L.R. Barreto), nataly.foronda@usp.br (N.F. Ortega), felipetlima@usp.br (F.T. Lima), avilapa@alumni.usp.br (P.A.Á.F. Carvalho), alexandre@ipef.br (A.V. Ferraz), jlmgonca@usp.br (J.L.M. Gonçalves).

https://doi.org/10.1016/j.tfp.2025.101053

Available online 17 October 2025

watersheds, reflecting the close relationship between water supply and productivity (Stape et al., 2004; Gonçalves et al., 2013; Steenhuis et al., 2023). This dynamic means that the selection of genotypes with varying yields within a watershed can significantly affect overall water consumption (Ferraz et al., 2019; Hubbard et al., 2020). Conversely, choosing the appropriate genotype for the local water conditions can mitigate or even avoid conflicts with other water users, contributing to water security and maintaining the balance between green and blue water.

Given the current environmental pressures and competition for water, a central challenge in forest management and tree breeding programs is to reconcile productivity with water conservation. Understanding how different genotypes perform under water-limited conditions is essential for selecting materials with optimal growth and water use traits (Câmara et al., 2020; Li et al., 2025). Selecting the right species and developing *Eucalyptus* genetic materials with an emphasis on water use efficiency are crucial for conserving water resources within watersheds where plantations are located (Barotto et al., 2017; Câmara et al., 2020; Ferreto et al., 2021). This requires a thorough understanding of the morphological traits and key physiological processes that control tree growth and their relationship with water use (Chen et al., 2020).

In particular, it is essential to comprehend and identify drought adaptation mechanisms, especially those involved in delaying dehydration in plants (Hakamada et al., 2017). Understanding how these mechanisms are activated and interact is vital for selecting drought-tolerant forest species, both for commercial cultivation and breeding programs (Paula et al., 2011; Gonçalves et al., 2017). Several studies have evaluated drought tolerance in *Eucalyptus*, identifying traits such as stomatal conductance, root system plasticity, and osmotic adjustment as key determinants of water use efficiency and survival under stress (Whitehead and Beadle, 2004; Chen et al., 2020). Additionally, environmental conditions, especially those related to water availability, also need to be considered when evaluating the water usage dynamics and drought-tolerance mechanisms. Evaluating water input into the soil, with variables such as effective precipitation (the amount of water that has reached the soil, considering throughfall and stemflow) and soil moisture, is an important aspect to understanding the water balance of a forest (Melo Neto et al., 2024), highlighting the effects of canopy and leaf traits on this input (Crockford and Richardson, 2000; Zhang et al., 2018).

Nonetheless, despite the growing body of literature on drought responses in Eucalyptus, comparative studies that link water use efficiency, transpiration, and growth across contrasting species remain limited. In Brazil, *Eucalyptus grandis* and *Eucalyptus urophylla* hold considerable silvicultural importance, especially regarding the supply of Brazilian strategic industries, such as pulp and paper, panels and energy. These species are among the most widely cultivated in Brazil and serve as the primary genetic sources for many clones (e.g. AEC-144 and H13, both widely used, from both from hybridization between *Eucalyptus grandis* and *urophylla*) used in commercial plantations nationwide (Gonçalves et al., 2009). Due to their growth and yield characteristics, as well as root system structure and drought-adaptation, *E. grandis* and *E. urophylla* are considered low and medium drought-resilient species according to the classification proposed by Gonçalves et al. (2013) and Gonçalves and Mello (2015), respectively. Therefore, expanding our knowledge on how species perform in terms of water use efficiency under different water availability conditions is essential for optimizing breeding programs and supporting management practices that enhance plantation productivity without compromising water resources (Saadaoui et al., 2017; Bouvet et al., 2020; Virtuoso et al., 2022).

However, understanding the water use efficiency of these species must involve comparisons with more drought-drought-resilient species, as breeding programs typically begin by identifying species that tolerate abiotic stresses, such as water deficits (Fonseca et al., 2010; Gonçalves et al., 2013). The most important *Eucalyptus* species in terms of water stress tolerance are predominantly found in the subgenus *Symphyomyrthus*, section *Exsertaria*, particularly *E. camaldulensis,* which is known as a drought-resilient species (Gonçalves et al., 2013; Gonçalves and Mello, 2015). The well-evolved tolerance mechanisms from this species were observed by Yousaf et al. (2018). This species has been widely utilized in hybridization programs, especially with *E. grandis*, resulting in highly promising clones for areas with severe water deficits (Gonçalves et al., 2013).

Genetic materials that are more tolerant to water deficiency often exhibit lower productivity due to the metabolic costs associated with tolerance mechanisms, such as stomatal regulation, production of osmoprotective compounds, and root system development (Whitehead and Beadle, 2004; Paula et al., 2011). While these physiological and morphological mechanisms help conserve water during critical periods of scarcity, they can negatively impact growth when water is abundant. Therefore, a major knowledge gap persists regarding the trade-offs between drought tolerance and productivity under different environmental conditions. Specifically, it remains unclear how transpiration and water use efficiency vary among species with contrasting drought responses, and how these factors influence wood yield. Addressing this gap is critical to improving genetic selection and guiding the deployment of clones suited to specific water availability scenarios (Kotowska et al., 2021; Climent et al., 2024). Thus, this study was based on the following hypothesis: Less drought-resilient species with higher growth rates, such as *E. grandis* and *E. urophylla*, consume more water through transpiration and are more efficient at using water for wood production than more drought-resilient species, such as *E. camaldulensis*, which has lower growth rates. To test this hypothesis, the study aimed to assess the growth and yield of *E. grandis* (low drought tolerance), *E. urophylla* (moderate drought tolerance), and *E. camaldulensis* (high drought tolerance) and their relationship with transpiration and water use efficiency.

2. Material and methods

2.1. Study area characterization

The study was conducted in a plantation established in March 2016 at the Experimental Station of Forest Sciences (EECF) in Itatinga, São Paulo, Brazil (23°10′ S, 48°40′ W, 860 m altitude). The local climate is classified as Cfa according to the Köppen classification system, characterized by a humid subtropical climate with an average annual temperature of 19 °C. The coldest months are June and July. Average annual rainfall is 1350 mm, with most precipitation occurring between October and March. However, an anomalous precipitation amount was observed during the period when the measurements were taken (August 2018 to July 2019), with a total annual precipitation of 2156 mm. The area's native vegetation is Cerrado. The terrain is flat, and the soil is classified as a typical medium-textured, dystrophic red-yellow latosol (EMBRAPA, 2012).

At the time of establishment, the soil was prepared in the planting lines with a subsoiler to a depth of 40 cm. Fertilization involved the application of the following nutrients in a continuous row (Lopes et al., 2022): 50 kg ha^{-1} of N, 26.2 kg ha^{-1} of P, and 100 kg ha^{-1} of K). Additionally, 2 t ha^{-1} of dolomitic limestone was applied to the surface to supply Ca and Mg. The first post-planting fertilization, conducted four months after planting, included the application of 20 kg ha^{-1} of N and 41.6 kg ha^{-1} of K. The second post-planting fertilization, conducted 10 months after planting, involved the application of 30 kg ha^{-1} of N, 66.5 kg ha^{-1} of K, and 5 kg ha^{-1} of B. Additional measures, such as weed and cutting ants control were done, with the latter being performed every semester to avoid potential tree damage.

Three plots were established using *E. grandis, E. urophylla*, and *E. camaldulensis*, species known for their low, medium, and high tolerance to water deficiency, respectively (Gonçalves et al., 2013; Gonçalves and Mello, 2015). Each plotconsisted of 38 rows with 10 trees per row (a total of 380 trees), with double-border planting and a 3 m x 3 m spacing

between rows and plants. Fig. 1 illustrates the plantation spatial arrangement as well as the destructive and non-destructive assessments. Each one of the species evaluated had a plantation area as the illustration, totalling three plantation areas. The plots are adjacent. Thirty-six trees from the measurable area of the plot (324 m^2) were used for non-destructive assessments, including forest inventory, transpiration, soil moisture, and leaf water potential measurements. The remaining rows were used for destructive sampling, such as biomass quantification.

2.2. Assessed variables

2.2.1. Growth and yield

Forest inventory measurements were taken within the measurable area of each species plot. Diameter at breast height (DBH), measured at 1.3 m above ground level, and height (H) were recorded for all trees at 12, 18, 27, 31, and 40 months after planting. Tree biomass quantification was performed at 11, 23, and 36 months after planting. In each plot, four trees were felled and sampled during the first two assessments, and eight trees per species were felled at 36 months (destructive sampling). Tree selection was based on DBH classes to ensure a representative sample from each class.

To estimate biomass, the trees were divided into stem wood, stem bark, branches, and leaves. Each component was weighed, and samples were taken for dry biomass estimation. The samples were dried at 65 °C until a constant weight was reached. Fresh and dry weights were used to determine moisture content and estimate total dry biomass for each tree compartment.

2.2.2. Climate data

Climate data, including atmospheric temperature, precipitation (total rainfall above canopy height), vapor pressure deficit (VPD), and relative humidity (RH), were collected from a meteorological station located approximately 1900 m from the study area at the experimental station.

2.2.3. Transpiration

Sap flow was quantified using the Granier (1985) method. Two cylindrical needles (probes) with a diameter of 2 mm and a length of 20 mm were used as sensors (a single sensor per tree). These sensors were inserted into the sapwood of the tree trunk at 1.3 m above ground level. The probes, fabricated following the guidelines of Delgado-Rojas (2003), were placed 2 cm deep into the stem. These two probes were placed with 10 cm between them. The upper probe was continuously heated, dissipating energy due to the Joule effect, while the lower probe was left unheated to measure the wood's actual temperature (reference temperature). The temperature difference between the two probes is inversely proportional to the sap flow density per unit of sapwood area (Granier et al., 1996).

To measure sap flow, six trees per species were selected based on the central DBH distribution classes, falling between −1 and +1 standard deviation from the mean. Since the original equation proposed by Granier (1985) tends to underestimate transpiration rates in *Eucalyptus* species, we applied calibrated Eqs. (1 and 2) from Delgado-Rojas (2008) for more accurate estimations.

$$k = \frac{\Delta Tmax - \Delta T}{\Delta T} \quad (1)$$

In which: ΔTmax (°C) = maximum temperature difference (°C) between the two measurement points (which usually occurs during the early morning), ΔT = current temperature difference (°C) between the two probes.

$$u = 478,017.10^{-6} k^{1,231} SA \quad (2)$$

In which: u = sap flow density ($m^3\ s^{-1}$), SA = sapwood area of the tree stem (m^2), and k = constant relating the flow density and the temperatures measured by the sensors.

The sapwood area (SA) of the trees was determined through destructive sampling conducted 36 months after planting for each species. Wood samples were collected at a height of 1.30 m from the base of the trees. The sapwood area was identified using a pressure system connected to a cylinder and compressor. Pressure was applied to a column of water mixed with Astra Violet dye, forcing the dyed water through the wood. The active sap-conducting area in the wood was stained by the dye. Discs approximately 1 cm thick were cut from the wood samples and scanned to estimate the sapwood area using ImageJ software.

The measured sapwood area was then correlated with the tree's circumference at breast height (CBH). A linear regression equation was fitted for each species based on these data. The sapwood area for the three species was estimated monthly using the constructed regression equations. The adjusted regression equations for *E. grandis* (Eq. (3)), *E. urophylla* (Eq. (4)), and *E. camaldulensis* (Eq. (5)) are provided below:

$$A_{Sap} = 3.499 * CBH - 67.03 \ \left(R^2 = 0922; p = 0.0006\right) \quad (3)$$

$$A_{Sap} = 2.396 * CBH - 39.07 \ \left(R^2 = 0923; p = 0.0006\right) \quad (4)$$

$$A_{Sap} = 4.277 * CBH - 72.43 \ \left(R^2 = 0926; p = 0.0005\right) \quad (5)$$

In which: A_{Sap} = sapwood area (cm^2), CBH = circumference at breast height (cm), R^2 = coefficient of determination, p = significance value of the F Test for linear regression. The sapwood area values in cm^2 were converted into m^2.

Individual tree transpiration was calculated using Eq. (2). The values were used to create a linear regression between individual tree transpiration and DBH for each day, using DBH as the independent variable. DBH measurements were taken within the plot for each species at 29, 32, 35, 38, and 41 months to monitor growth. We subsequently applied the

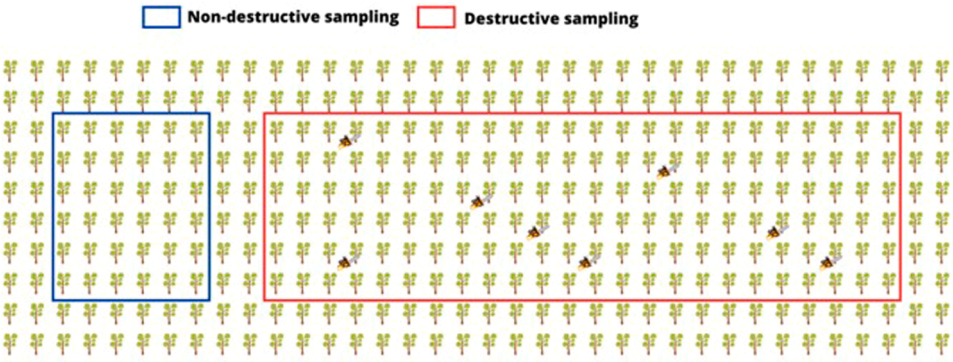

Fig. 1. Spatial layout of the experimental plots showing the arrangement of trees. Trees designated for non-destructive sampling are highlighted in blue, while trees selected for destructive sampling.

regression to estimate individual tree transpiration for every tree in the stand. The sum of transpiration for all trees in the stand in each day is given in m^3 day^{-1}, which multiplied by 1000 is L day^{-1}. Daily stand transpiration was divided by the total area of the plot to obtain the values in mm day^{-1}.

2.2.4. Leaf area index (LAI)

The leaf area (LA) of individual trees was quantified annually through destructive sampling conducted at 11, 23, and 36 months after planting. The same trees felled and used for biomass assessment were also used for leaves sampling. Therefore, four trees had their leaves sampled in each of the first two assessments, and eight trees per species were sampled at 36 months, totalling 16 trees for each species for leaves sampling. Each sampling was performed during the same period of the year (wet season). In each assessment, 30 leaves were collected from the bottom, middle, and top sections of the canopy. The fresh weight of these samples was recorded, and the leaves were scanned for area determination using the ImageJ software. After scanning, the samples were dried at 65 °C until a constant weight was achieved, and their dry weight was measured. Specific leaf area (SLA) was calculated by dividing the scanned area by the dry mass of the leaves. The LA of individual trees was then estimated by multiplying the SLA by the total dry weight of leaves per tree.

To estimate the LA for all trees in the plot, linear mixed-effects models were fitted for each species (Table 1, Eq. (6)). Based on these models, LA (m^2) was estimated for all trees at 12, 18, 27, and 31 months after planting. The leaf area index (LAI, m^2 m^{-2}) was calculated by summing the LA of all trees for each measurement period and dividing it by the total area of the subplots. To account for the variation between trees sampled in different years, "year" was included as a random effect in the leaf area model. Due to the use of log transformations for the response variable and further use of Eq. (6) to estimate individual tree leaf area for the remaining trees in the stand, the correction factor by Baskerville, 1972 was used to avoid bias, a similar approach than that used by de Castro Segtowich et al. (2025), to estimate leaf area.

$$\log(leaf\ area) = intercept + \log(dbh)*a \quad (6)$$

In which, leaf area, when back transformed, is in m^2; dbh in its original unit is in cm; a is a coefficient.

2.2.5. Environmental variables

2.2.5.1. Effective precipitation. Effective precipitation (EP), known as the rainfall that effectively reaches the soil, was calculated by summing throughfall (T) (Eq. (7)) and stemflow (Et) (Eq. (8)). To determine throughfall (T), the average values from nine rain gauges installed at 1.5 m above ground level were used. The rain gauges were evenly distributed within the plot to capture representative measurements of rainfall that passed through the canopy.

$$T = \frac{V}{A}*10 \quad (7)$$

In which: T = throughfall (mm); V = Water volume collected at the pluviometer (mL); A= Pluviometer caption area (cm^2).

Additionally, stemflow (Et) was quantified by installing four water collection and storage systems for each species. These systems consisted of hoses attached to the tree trunks, which directed the water into 50-liter plastic containers. The stemflow (Et) was calculated using the following equation:

$$Et = \frac{V}{A} \quad (8)$$

In which: Et = Stemflow (mm); V =Volume of water collected (L); A = Projected area of the canopy (m^2), which was considered to be 9 m^2.

2.2.5.2. Soil moisture. Soil moisture monitoring was carried out using a capacitive Frequency Domain Reflectometry (FDR) probe, model DIVINER. Gravimetric moisture (Ug) and soil density (Ds) were determined from soil samples collected at various depths using volumetric rings to calibrate the probe. A representative tree (present in the interval between +1 and −1 standard deviation), from each species within the measurable area was selected from the forest inventory, next to which three access tubes were installed: one in the subsoiling line (between trees), one between the rows, and one at the intersection of the quadrant formed with neighboring trees, totaling three tubes per species in the measurable area. The tubes were installed to a depth of 1.60 m, and readings were taken every 10 cm.

2.2.6. Leaf water potential (Ψ_{leaf})

Leaf water potential (Ψleaf) was assessed monthly over a 12-month period, beginning at 28 months after planting. Four trees with average DBH were selected from the measurable area for each species. Scaffolds were installed—one for each species—to facilitate access to the upper canopy. Readings were taken from fully expanded leaves in the upper third of the canopy. The leaves were sampled from four trees in each species, to allow the measurement using a Scholander-type pressure chamber, model 600 (Soil Moisture Equipment Corp., Santa Bárbara, Califórnia-USA). Readings were taken pre-dawn (≈ 3:30 a.m. – 5:30 a.m.) and at midday (≈ 12:00 noon – 2:30 pm.).

2.2.7. Water use efficiency (WUE)

Monthly assessments of trees equipped with sap flow sensors included measuring DBH growth using a measuring tape. Based on DBH and dry stem wood biomass values from the destructive sampling performed at 36 months post-planting, an equation was fitted to estimate the increase in stem wood biomass over a 12-month period for all three species (Table 2, Eq. (10)). Water use efficiency (WUE) was calculated as the ratio between the increase in stem wood biomass and the volume of water transpired during the same period (Eq. (9)). Since our focus primarily lies on the relationship between wood productivity and water usage, we prioritized stem wood biomass increment for calculating WUE.

Table 1
Linear mixed-effects models used for predicting leaf area (LA) for the three *Eucalyptus* species (*E. grandis, E. urophylla*, and *E. camaldulensis*). The models were fitted using DBH as the predictor variable, while "year" was included as a random effect to account for the variability in sampling periods across different years.

Model	Response variable	Parameters	Estimates	Std. Error	p value
Eucalyptus grandis	log (LA)	log (dbh)			
		intercept	−0.83641	0.643815	0.2183
		a	1.93791	0.228403	< 0.0001
Eucalyptus urophylla	log (LA)	log (dbh)			
		intercept	−0.44061	0.776792	0.581
		a	1.72512	0.354402	4.00E-04
Eucalyptus camaldulensis	log (LA)	log (dbh)			
		intercept	1.05437	0.686699	0.1506
		a	0.99311	0.32909	0.0107

Table 2
Non-linear models used to predict dry stem wood biomass (kg) for the three *Eucalyptus* species (*E. grandis, E. urophylla*, and *E. camaldulensis*). The models were fitted using DBH as the predictor variable, with species-specific equations developed to provide accurate biomass estimations across different growth stages.

Model	Response variable	Parameters	Estimates	Std. Error	p-value
Eucalyptus grandis	Stem wood (kg)	dbh (cm)			
		a	0.3503	0.3503	0.29859
		b	1.9031	0.3226	0.00105
Eucalyptus urophylla	Stem wood (kg)	dbh (cm)			
		a	0.0807	0.04877	0.149
		b	2.40096	0.22045	3.55E-05
Eucalyptus camaldulensis	Stem wood (kg)	dbh (cm)			
		a	0.2991	0.2213	0.22533
		b	1.7959	0.3051	0.00107

$$WUE = \frac{\Delta Biomass}{Transpiration} \quad (9)$$

In which: WUE = Water use efficiency in g of dry stem wood dry weight biomass l^{-1}, for tree-level WUE and kg mm^{-1} day^{-1} ha^{-1}, for stand-level WUE; ΔBiomass = Final biomass - Initial biomass (g), Transpiration (L on tree-level and mm on stand-level).

$$Stem\ wood = a \times \left(dbh^{b}\right) \quad (10)$$

In which, stem wood corresponds to the dry weight of stem wood in kg; dbh is in cm; a and b are coefficients.

2.3. Data analysis

The Kruskal-Wallis non-parametric test was used at a significance level of 0.05, along with the Bonferroni correction, to compare transpiration, effective precipitation and water use efficiency (WUE) among the three *Eucalyptus* species (*E. grandis, E. urophylla*, and *E. camaldulensis*), considering both wet and drier seasons. The choice of a non-parametric test was based on the fact that the data did not meet the assumptions required for an ANOVA test, as previously observed in a similar study by Lopes et al. (2022) conducted in the same area. All statistical analyses were performed using R software (R Core Team, 2022). Figures were generated using the 'ggplot2' package in R, as well as SigmaPlot 15.0.

3. Results

3.1. Trees growth and yield

E. grandis exhibited the highest DBH values throughout the evaluation period (12 to 40 months after planting), followed by *E. urophylla* and *E. camaldulensis* (Fig. 2). *E. grandis* also showed greater height across the entire period. At 40 months, the average DBH for E. grandis was 4.8 % and 29 % higher than that of *E. urophylla* and *E. camaldulensis*, respectively. In terms of height, E. grandis was 18 % taller than *E. urophylla* and 41 % taller than *E. camaldulensis*. Notably, the difference in DBH growth between *E. urophylla* and *E. camaldulensis* became more pronounced over time. Regarding height, the divergence between *E. urophylla* and *E. camaldulensis* only emerged between 18 and 27 months after planting (Fig. 2). At 27 months, *E. urophylla* was, on average, 29 % taller than *E. camaldulensis*.

Although no significant difference was observed for any assessment periods, *E. urophylla* had the highest average total dry biomass 11 months after planting, with values 0.4 t ha^{-1} higher than *E. grandis* and 1.4 t ha^{-1} higher than *E. camaldulensis* (Fig. 3). However, 12 months later, *E. grandis* surpassed the other species, with total biomass 13.7 t ha^{-1} greater than *E. urophylla* and 24.1 t ha^{-1} greater than *E. camaldulensis*. This trend continued at 36 months, with *E. grandis* reaching an average of 71.7 t ha^{-1} of dry biomass. Regarding biomass allocation across the different aboveground compartments, *E. grandis* showed higher stem wood and biomass than *E. camaldulensis* 36 months after planting. In general, for all species, there was a greater allocation of biomass to the stem wood and bark after 23 months, compared to other compartments.

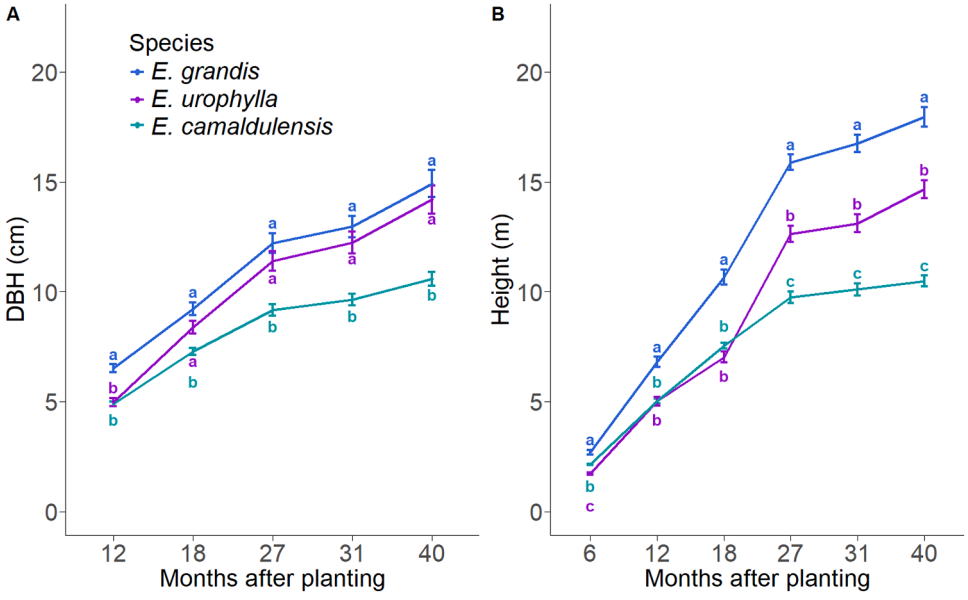

Fig. 2. Diameter at breast height (DBH) (A) and height (B) as a function of months after planting for the three *Eucalyptus* species. Error bars represent the standard error of the mean DBH and height for all trees within the measurable areas. Species followed by the same letter (in the same month) do not differ significantly according to the Kruskal-Wallis test with Bonferroni correction (Wilcox test) at $p = 0.05$.

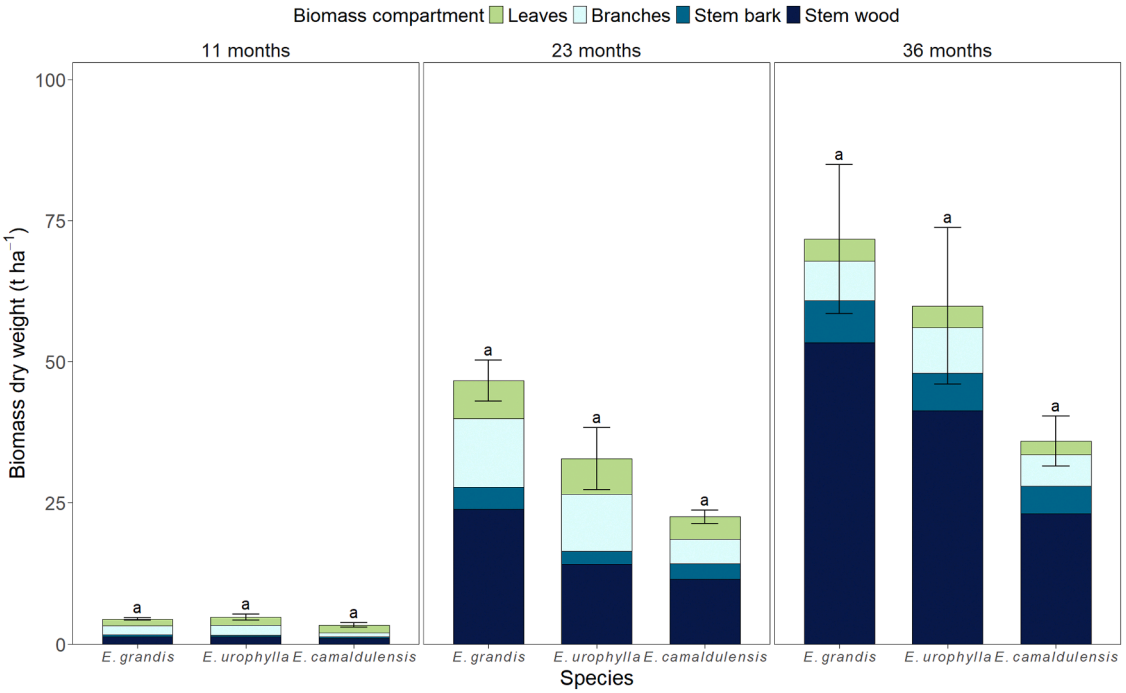

Fig. 3. Aboveground biomass (stem wood, bark, leaves, and branches) at different ages of the stands (11, 23, and 36 months after planting) for the three Eucalyptus species. Numbers in parentheses represent the standard error. Error bars represent the standard error of the total for the number of sampled trees ($N = 4$ at 11 and 23 months; $N = 8$ at 36 months). Bars with the same letter within the same age do not differ significantly according to the Kruskal-Wallis test with Bonferroni correction (Wilcox test) at $p = 0.05$.

3.2. Ecophysiological variables

3.2.1. Transpiration and leaf water potential (Ψ_{leaf})

Significant differences in stand-level transpiration between the drier and wet seasons were found only for *E. grandis* ($p = 0.0103$) and *E. camaldulensis* ($p = 0.02$) (Fig. 4), with both species showing higher transpiration during the wet season. In contrast, *E. urophylla* did not show a significant difference between the two seasons ($p = 0.0921$), with total transpiration values of 345 mm during the wet season and 294 mm during the drier season. When comparing species within each season, differences were observed during the wet season: *E. grandis* exhibited the highest stand-level transpiration values, while *E. camaldulensis* showed the lowest. In the drier season, *E. grandis* again displayed the highest stand-level transpiration rates, differing from *E. urophylla* ($p = 0.015$). However, *E. camaldulensis* did not differ from either of the other species during the drier season ($p > 0.05$).

When evaluating the species' stand-level transpiration over the months, *E. grandis* consistently exhibited the highest transpiration values throughout the entire evaluation period, with a more pronounced difference from the other species between December 2018 and January 2019, the warmest months (Fig. 5). *Eucalyptus camaldulensis* showed higher transpiration rates than *E. urophylla* starting in October 2018, with a particularly marked difference between March and May 2019. Finally, the differences in transpiration among the three species diminished considerably from June 2019 onward (Fig. 5).

E. urophylla showed the lowest Ψ_{leaf} values in almost all measurements, except for June during the early morning, when *E. camaldulensis* exhibited the most negative Ψ_{leaf}. *E. grandis* had the highest Ψ_{leaf} values

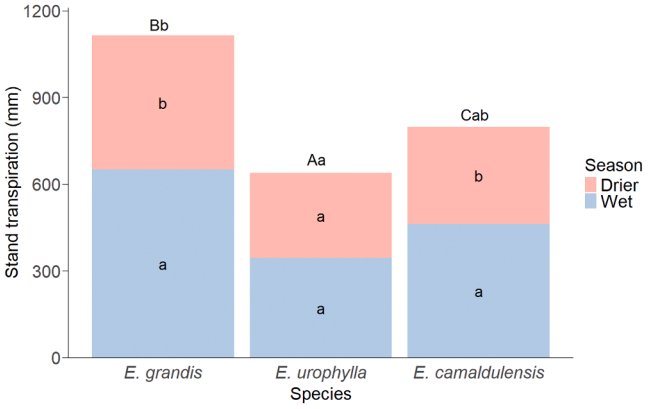

Fig. 4. Stand-level transpiration of three *Eucalyptus* species during the drier period (April to September) and the rainy season (October to March). Letters within the columns compare transpiration between the two seasons for each species. Uppercase letters above the columns represent comparisons among species during the rainy season, while lowercase letters represent comparisons during the drier period. Columns followed by the same letter do not differ significantly according to the Kruskal-Wallis test with Bonferroni correction (Wilcox test) at $p = 0.05$.

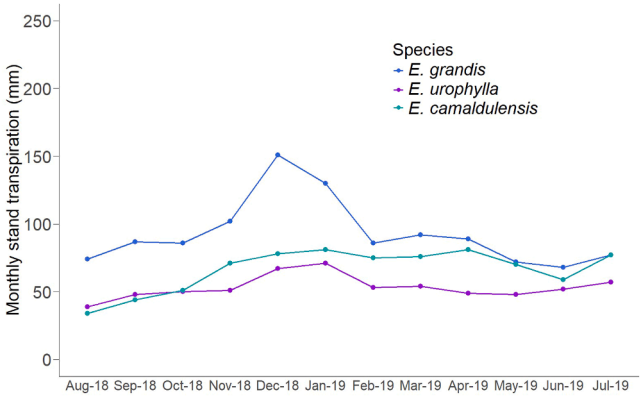

Fig. 5. Stand-level transpiration of *Eucalyptus* species as a function of months after planting.

in most measurements. The peak of Ψ_{leaf} values were recorded in February 2019 (the wettest month of the study) at dawn, with potentials of −0.064 MPa for *E. grandis*, −0.067 MPa for *E. camaldulensis*, and −0.072 MPa for *E. urophylla* (Fig. 6). The lowest Ψ_{leaf} values were observed at midday in July 2018 (the driest month), with readings of −1.054 MPa for *E. grandis*, −1.688 MPa for *E. camaldulensis*, and −1.984 MPa for *E. urophylla* (Fig. 7). The highest Ψ_{leaf} values were recorded in February 2019. In terms of vapor pressure deficit (VPD), the maximum values at both pre-dawn and midday occurred in December 2018, while the lowest were observed in February 2019.

For the three assessed *Eucalyptus* species, Ψ_{leaf} and VPD values exhibited a strong negative correlation (Fig. 8). *E. urophylla* stood out as the most sensitive species to changes in Ψ_{leaf} compared to the others, which can be explained by the steeper angular coefficient in the correlation analysis. High correlations were also found between Ψ_{leaf} and relative humidity (RH) (Fig. 9), with *E. urophylla* displaying the greatest variation in Ψ_{leaf} in response to RH. These results highlight the direct influence of VPD and RH on Ψ_{leaf} values in the three species, with *E. urophylla* showing the highest sensitivity to fluctuations in both variables.

3.2.2. Leaf area index

All three *Eucalyptus* species exhibited an increase in Leaf Area Index (LAI) over time during the wet period. *Eucalyptus grandis* consistently showed the highest LAI values in all measurement periods. Although *Eucalyptus urophylla* had the lowest LAI at 12 months, it demonstrated significant growth in this variable, reaching the second highest LAI throughout the study period. From 18 months after planting onward, *E. camaldulensis* had the lowest LAI values (Fig. 10).

3.3. Environmental assessments

3.3.1. Effective precipitation

Although higher Effective Precipitation (EP) values were observed during the wet season, no significant differences were found between the two seasons within each species (Fig. 11). Similarly, no differences in EP were detected when comparing the species, regardless of the season.

3.3.2. Soil moisture

Soil Moisture up to a depth of 1.60 m varied considerably throughout the study period (Fig. 12). *E. urophylla* consistently had higher soil moisture in the top layer (0–30 cm) during most of the evaluation period. Between January 8 and January 24, 2019, a sharp decrease in soil moisture was observed. During this period, the soil under *E. grandis* showed a more pronounced reduction in moisture in the 30–160 cm layer (an average of 39 mm), compared to the soil under *E. urophylla* (30 mm) and *E. camaldulensis* (28 mm). Notably, during the same period, total precipitation was only 23 mm, while all three species transpired more than the amount of precipitation.

3.4. Water use efficiency (WUE)

When comparing the average individual tree WUE between the dry and wet seasons for each species, only *E. camaldulensis* showed a significant difference, with higher WUE during the drier period compared to the wet period (Fig. 12). Among the species within each season (Fig. 13), *E. urophylla* exhibited the highest individual tree WUE in both the drier and wet seasons, while *E. camaldulensis* had the lowest. Specifically, during the drier season, *E. urophylla* had an average WUE of 3.4 ± 0.4 g L^{-1}, followed by *E. grandis* (1.7 ± 0.4 g L^{-1}) and *E. camaldulensis* (0.8 ± 0.1 g L^{-1}). In the wet season, *E. urophylla* had a WUE of 4.0 ± 0.6 g L^{-1}, *E. grandis* 2.4 ± 0.5 g L^{-1}, and *E. camaldulensis* 0.5 ± 0.1 g L^{-1}.

E. urophylla exhibited the highest stand WUE throughout the assessment period, peaking between August 1st and September 26th at 1.75 kg mm^{-1}, followed by *E. grandis* (0.89 kg mm^{-1}) and *E. camaldulensis* (0.47 kg mm^{-1} ha^{-1}) (Fig. 14). *E. camaldulensis* consistently showed the lowest WUE values over the entire evaluation period. When calculating stand WUE for the entire period (August 1st, 2018 – July 25th, 2019), *E. urophylla* presented the highest WUE (0.94 kg mm^{-1}), which was 33 % and 79 % higher than that of *E. grandis* (0.63 kg mm^{-1}) and

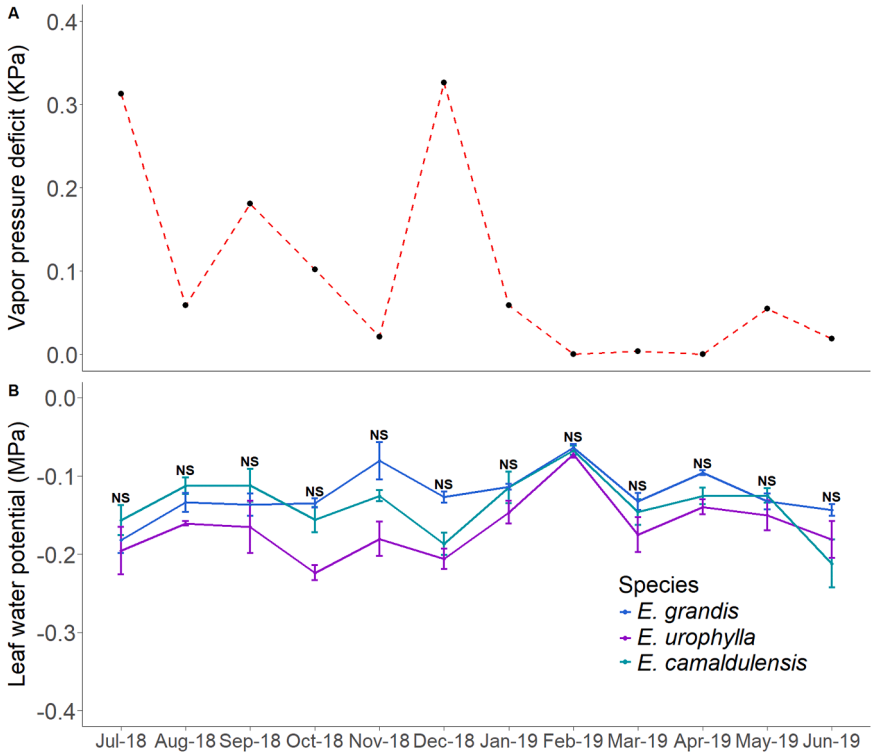

Fig. 6. Average leaf water potential (MPa) and vapor pressure deficit (VPD, kPa) values for each *Eucalyptus* species measured between 3:30 a.m. and 5:30 a.m. Error bars represent the standard error of the four trees sampled in each measurable area. NS: non-significant according to the Kruskal-Wallis test $p = 0.05$.

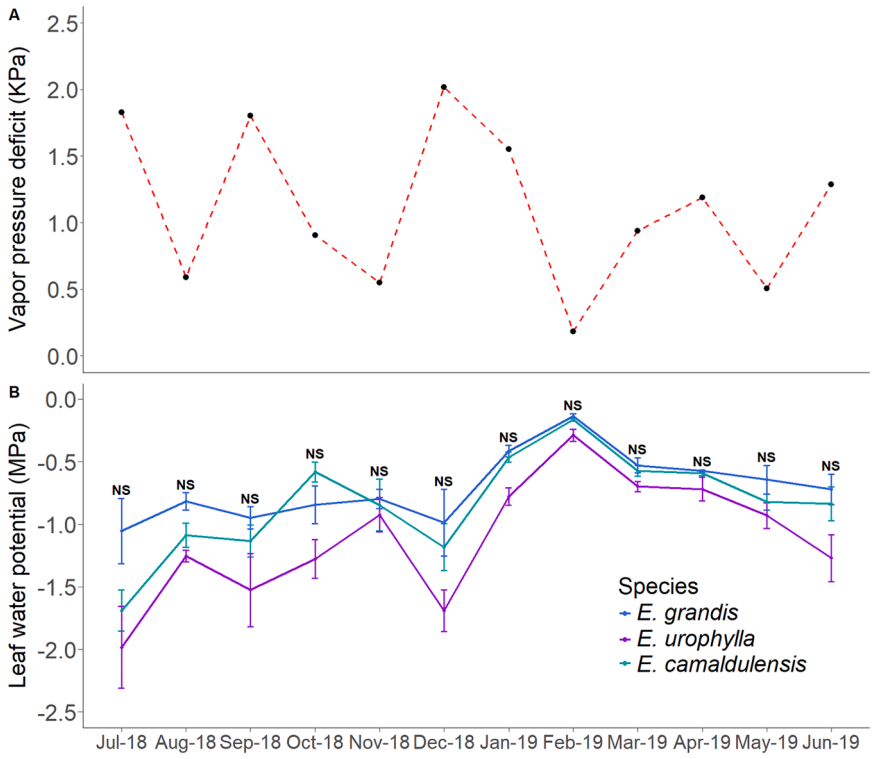

Fig. 7. Average leaf water potential (MPa) and vapor pressure deficit (VPD, kPa) values for each *Eucalyptus* species measured between 12:00 noon and 2:30 pm. Error bars represent the standard error of the four trees sampled in each measurable area. NS: non-significant according to the Kruskal-Wallis test $p = 0.05$.

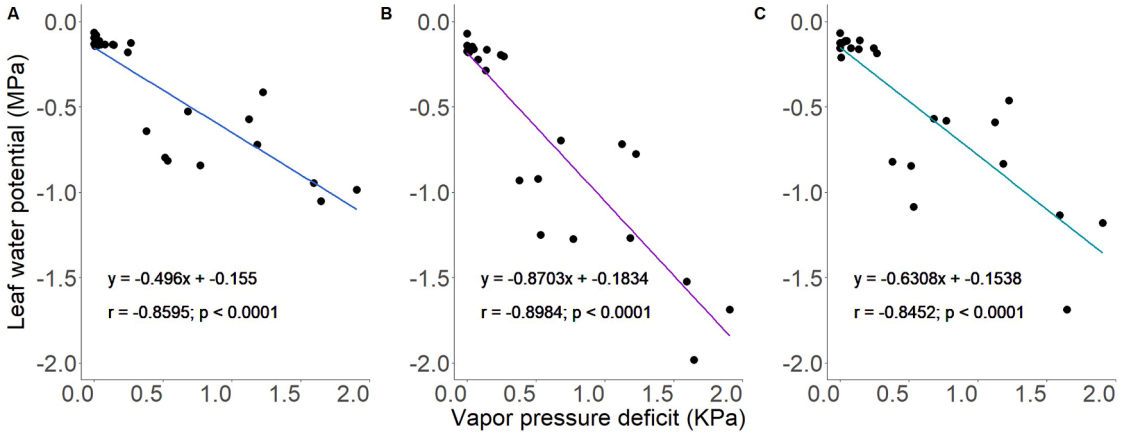

Fig. 8. Regression between leaf water potential (Ψ_{leaf}) (values from both 12:00 noon and 2:30 pm. assessments) and vapor pressure deficit (VPD) for *E. grandis* (A), *E. urophylla* (B), and *E. camaldulensis* (C).

E. camaldulensis (0.19 kg mm^{-1}), respectively.

When evaluating the DBH of the trees used for sap flow analysis in the transpiration measurements (Fig. 15), *E. grandis* consistently showed the highest values throughout the measurement period, followed by *Eucalyptus urophylla* and *E. camaldulensis*, respectively, corroborating the results observed for the entire stand (Fig. 2).

4. Discussion

Drought-resilient species often allocate resources to stress tolerance mechanisms at the expense of competitive growth under optimal conditions, compared to less tolerant species (Zhang et al., 2020). In line with this, *E. camaldulensis*, a species known for its ability to adapt to water stress conditions (Quiñones-Martorello et al., 2023), showed lower growth rates under the low water limitation conditions of this study, followed by the moderately drought-resilient *E. urophylla* and the less drought-resilient *E. grandis* (Fig. 2).

In *Eucalyptus* species, water and nutrient stress tends to be more critical during the early stages of development (Gonçalves et al., 2013). Species such as *E. camaldulensis*, which efficiently utilize tolerance mechanisms like rapid root growth (Saadaoui et al., 2017), may exhibit higher initial growth rates than less adapted species, even under favorable soil and climate conditions, which is likely due to the faster root establishment in the early stage (Yousaf et al., 2018; Ávila, 2020). This trend was observed in the present study, despite *E. camaldulensis* ultimately showing lower height and DBH values at the end of the assessment. Another study conducted at the same site has shown that *E. camaldulensis* had proportionally greater root system biomass compared to *E. grandis* and *E. urophylla* up to 36 months after planting, resulting in a higher below-ground to above-ground biomass ratio

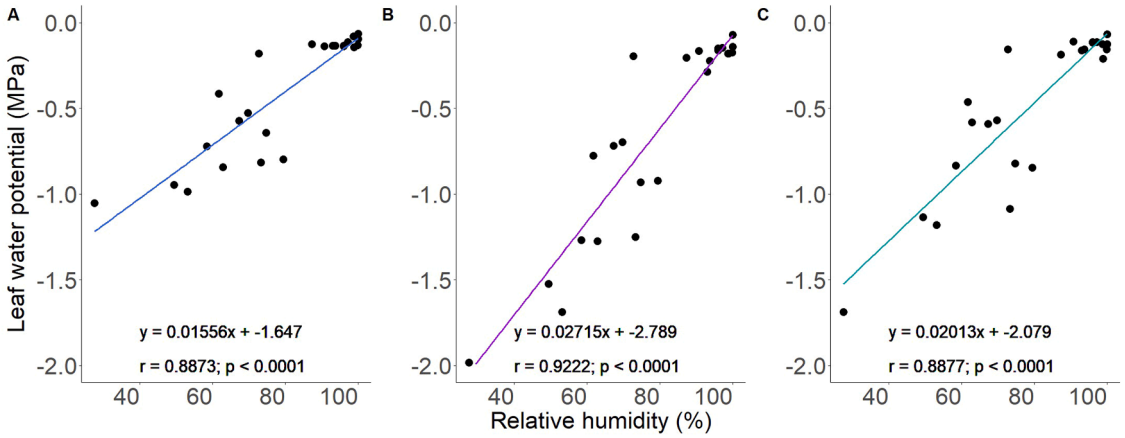

Fig. 9. Regression between leaf water potential (Ψ_{leaf}) (values from both 12:00 noon and 2:30 pm. assessments) and relative humidity (RH) for *E. grandis* (A), *E. urophylla* (B), and *E. camaldulensis* (C).

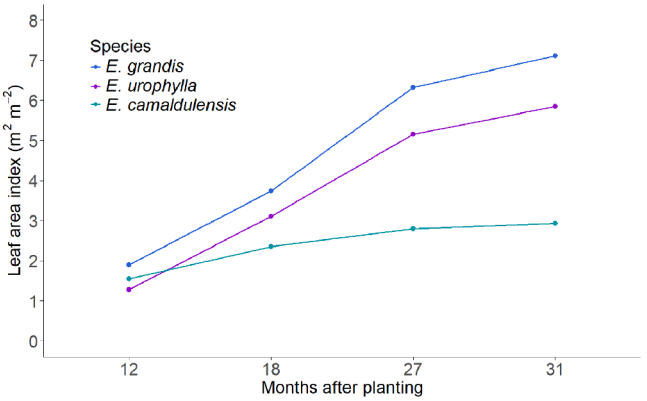

Fig. 10. Leaf area index (LAI) for each *Eucalyptus* species as a function of months after planting.

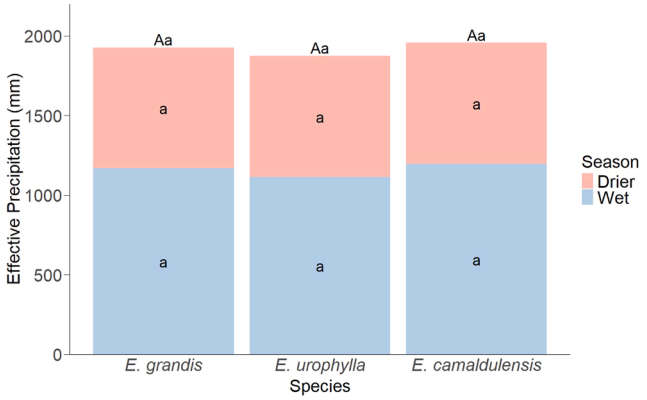

Fig. 11. Effective precipitation (EP) for three *Eucalyptus* species during the period (April to September) and the rainy season (October to March). Letters within the columns compare the two seasons for each species. Uppercase letters above the columns represent comparisons among species during the rainy season, while lowercase letters represent comparisons during the drier period. Columns followed by the same letter do not differ significantly according to the Kruskal-Wallis test with Bonferroni correction (Wilcox test) at $p = 0.05$.

(Ávila, 2020). This ratio, which reflects a plant's strategy for adapting to soil water availability, can vary depending on the *Eucalyptus* species (Pinheiro et al., 2016). These aspects are, therefore, vital to understand the relationship between water consumption and growth (notably, stem wood biomass production), and how the greater biomass growth may represent a more efficient water consumption in some situations, as stated by the hypothesis of the present study.

Higher transpiration values during the wetwet season suggest that plants tend to transpire more in periods of increased temperature, vapor pressure deficit (VPD), and photoperiod (Dye et al., 2001), as observed particularly for *E. grandis* and *E. camaldulensis* (Fig. 4). On the other hand, the low seasonal variation in the transpiration of *E. urophylla* is a recognized and well-documented feature in the literature on the species, along with its generally lower transpiration rates compared to other tree species (Abreu et al., 2022; Herrera et al., 2012). Notably, *E. urophylla* exhibited lower transpiration rates than native South American savannah species such as *Trachypogon vestitus* and *Curatella americana* (Herrera et al., 2012), with minimal variation in CO_2 fixation rates. These findings align with previous studies (e.g. Santos and Balbuena, 2017) and suggest that *E. urophylla* is a promising species for carbon sequestration with minimal impact on soil water balance. The variation in transpiration rates of *E. camaldulensis*—similar to *E. grandis* during the wet season but closer to *E. urophylla* during other periods—reached its lowest value in October, highlighting the species' strong adaptation to water stress (Fig. 4). *E. camaldulensis* plantations subjected to prolonged water deficits have been shown to exhibit significantly lower transpiration rates (Engel et al., 2005; Doody et al., 2015), lower than those observed in this study. However, because the conditions in this study were not highly water-restricted, *E. camaldulensis* did not fully engage its drought tolerance mechanisms, which could have reduced water loss to an even greater extent.

Regarding biomass production, *E. grandis* and *E. urophylla* are both highly productive under the conditions of this study, consistent with findings from other researches involving these species (e.g., Abreu et al., 2022; Mariño Macana et al., 2022; Masullo et al., 2022; Rocha et al., 2019; Santos and Balbuena, 2017). On the other hand, *E. camaldulensis*, known for its greater tolerance to water stress, exhibits slower growth as part of its strategy to minimize water loss (Lemcoff et al., 2002; Yang et al., 2018). The results of this study suggest that this lower biomass production persists for *E. camaldulensis*, even when grown under conditions with minimal water limitation, corroborating the hypothesis stated by the present study.

Such hypothesis is strengthened when we observe the relationship between biomass production and transpiration (namely, WUE). The smaller variation in WUE values between *E. camaldulensis* and the other species during the drier season, combined with its well-documented adaptation abilities (Quiñones-Martorello et al., 2023; Saadaoui et al., 2017), suggests that *E. camaldulensis* may achieve higher WUE under severe water stress, potentially surpassing the other species evaluated (Fig. 11). However, the lower DBH growth of *E. camaldulensis*

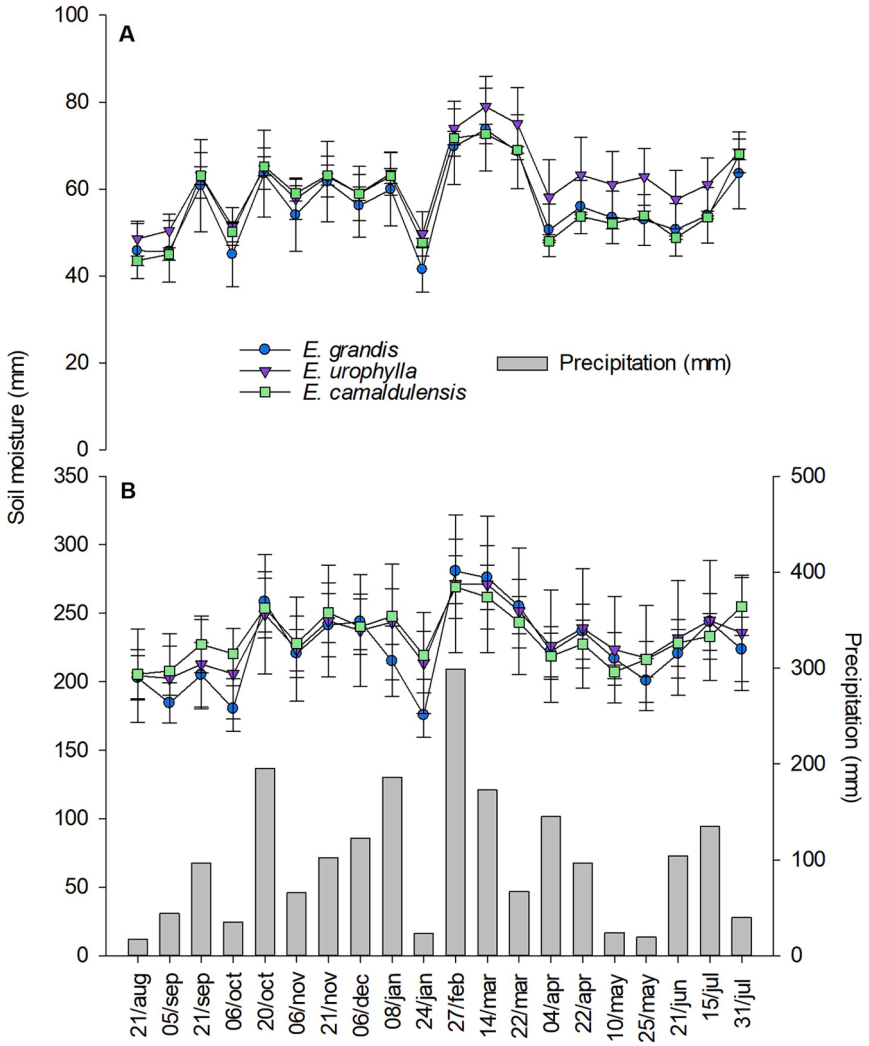

Fig. 12. Soil moisture (mm) in the 0–30 cm (A) and 30–160 cm (B) layers, and total precipitation (mm) for each *Eucalyptus* species between 21/08/2018 and 31/07/2019. Vertical bars next to the data points represent the standard error of the mean.

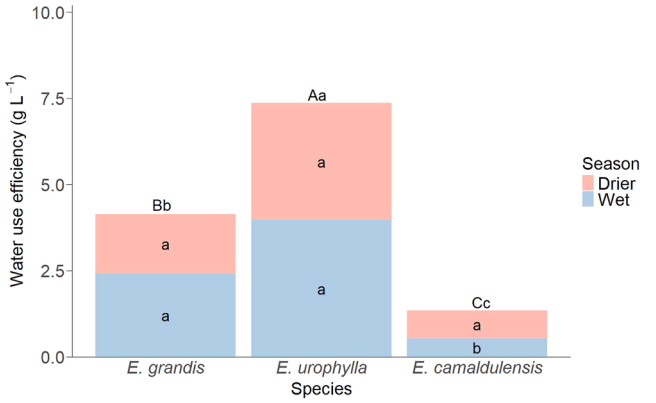

Fig. 13. Tree-level water use efficiency (WUE; stem biomass/transpired water) for each *Eucalyptus* species during the drier season (April to September) and the rainy season (October to March). Letters within the columns compare WUE between the two seasons for each species. Uppercase letters above the columns represent comparisons among species during the rainy season, while lowercase letters represent comparisons during the drier season. Columns followed by the same letter do not differ significantly according to the Kruskal-Wallis test with Bonferroni correction (Wilcox test) at $p = 0.05$.

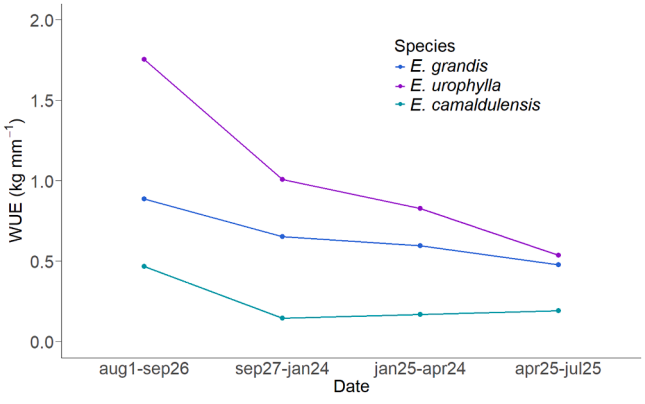

Fig. 14. Water use efficiency (WUE), represented by the ratio between the increase in wood biomass and the amount of water transpired, from August 2018 to July 2019.

underscores its reduced investment in net primary biomass productivity. In contrast, *E. urophylla*, which had the highest WUE over the entire evaluation period, also exhibited high DBH growth, reinforcing its potential as a highly productive and water-efficient species, which is closely related to its lower growth and biomass production. the WUE

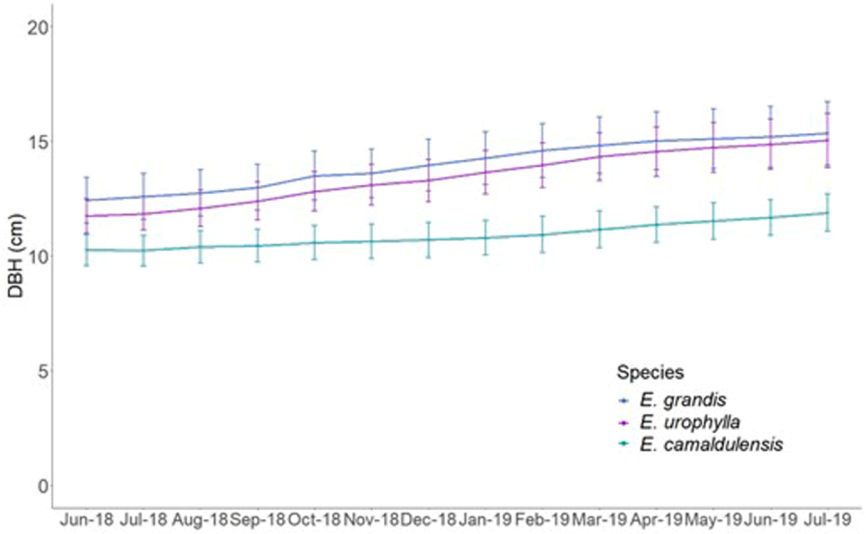

Fig. 15. Diameter at breast height (DBH) of *Eucalyptus* species trees selected for sap flow measurements.

values observed for *E. camaldulensis* during the wet season, which are likely due to the increased water availability, leading to higher water uptake by this species, which is supported by *E. camaldulensis* exhibiting the second-highest transpiration rate but the lowest growth rate among the species evaluated (Fig. 10), confirming again our hypothesis.

Nonetheless, it is worth mentioning the highest WUE for *E. camaldulensis*, which was recorded during the drier season, indicating that this species primarily activates its water stress tolerance mechanisms when water availability is lower (Doody et al., 2015). Additionally, *E. camaldulensis* is capable of developing fine roots in deeper soil layers to access water as needed. Ávila (2020), in a study of *Eucalyptus* root systems of similar age, found that *E. camaldulensis* produced a greater accumulated root length from the surface down to 3 m compared to *E. grandis* and *E. urophylla*. Despite its lower growth, *E. camaldulensis* had a similar fine root density in the deeper layers as less drought-resilient species. The higher proportion of fine roots in deeper soil layers relative to above-ground biomass enhances the species' ability to adapt to water stress (Gonçalves et al., 2013; Christina et al., 2017). Conversely, the higher WUE values observed for *E. urophylla*, particularly during the wet season, are consistent with its lower transpiration rates and its position as the species with the second-highest growth rate.

Tree growth under temporary water stress conditions is closely tied to the ability of stomata to regulate water loss while maintaining growth (Lima et al., 2003; Chen et al., 2020). Stomatal closure is the primary response to water stress, aiming to reduce water loss and prevent declines in xylem and leaf water potential (Martorell et al.,. 2014). Although Ψ_{leaf} alone is not a direct indicator of stomatal activity (Gollan et al., 1985), it is closely related to transpiration and stomatal regulation. Consequently, stomatal functioning plays a crucial role in controlling transpiration rates under conditions of high temperatures and low relative humidity, making stomatal closure an essential strategy for avoiding excessive water loss (Figs. 7 and 8), which is closely linked to the leaf area and water potential. The high Ψ_{leaf} values recorded at dawn, all above −0.3 MPa (Fig. 5), indicate that none of the species were experiencing severe water stress, as drought tolerance tends to increase with more negative pre-dawn Ψ_{leaf} values (Sivananthawerl and Mitlohner, 2003). Hakamada et al. (2017) reported that Ψ_{leaf} values for *E. urophylla* could reach −1.7 MPa under water stress, suggesting that the Ψ_{leaf} of the species in this study could become more negative under more severe drought conditions.

The higher soil moisture values observed for *E. urophylla* and the lower values for *E. grandis* (the species with the lowest and highest transpiration rates, respectively) indicate an inverse relationship between soil moisture and tree transpiration. In January, when soil moisture decreased, the elevated transpiration rates of all three species, particularly *E. grandis*, suggest that the rate of water extraction by the trees likely exceeded the rate of replenishment from rainfall, leading to the observed decline in soil moisture (Fig. 9). Despite *E. urophylla* showing higher soil moisture content, it had lower effective precipitation levels, while *E. camaldulensis* presented the highest effective precipitation. This is related to the higher LAI values in *E. urophylla* and lower LAI in *E. camaldulensis*. These results also highlight the efficiency of *E. urophylla* in maintaining elevated soil moisture levels despite its high LAI (Fig. 10).

The high water availability in this study site contributed to the high LAI values observed for all species across all assessment periods. In contrast, Battaglia et al. (1998) reported a linear decrease in LAI under water stress in *Eucalyptus nitens* and *Eucalyptus globulus* plantations. *E. grandis* can maintain approximately 40 % of its maximum stomatal conductance (Gs) at Ψ_{leaf} values below −2.45 MPa (Mielke et al., 2000), suggesting that its lower stomatal control likely contributes to its higher transpiration rates compared to *E. urophylla*, particularly at midday (Fig. 6). Whereas *E. urophylla* can sustain 50–60 % of its maximum Gs at Ψ_{leaf} values of −1.6 MPa (Zhang et al., 2016), demonstrating high water use efficiency, even when water availability is not significantly restricted, as observed in this study.

Doody et al. (2015) found that *E. camaldulensis* typically maintains a leaf area index (LAI) above 0.5 m^2 m^{-2} under moderate water stress conditions. A reduction in LAI below 0.5 m^2 m^{-2} indicates a significant response to drought, as observed in areas with severe water scarcity (Doody et al., 2015). Conversely, at our study site, *E. camaldulensis* maintained LAI values above 1 m^2 m^{-2}. Fast-growing species generally exhibit high transpiration rates, with transpiration regulation reflecting various tolerance mechanisms in response to environmental changes (White et al., 2000). *E. grandis*, which had the highest growth rates among the species evaluated, also showed consistently high transpiration rates, particularly during the warmer months. Furthermore, *E. grandis* maintained the highest LAI values throughout the study, which likely contributed to its elevated transpiration rates.

Christina et al. (2017) described a drought escape mechanism in trees, involving water extraction from deeper soil layers while continuing to produce biomass. This mechanism consists of deep root development in the early stages of growth, before canopy closure, even when there is sufficient water in the surface layers to meet plant demand. This adaptation prepares trees for potential water shortages later

in the year. However, these authors pointed out that once the canopy closes, the amount of water transpired by plants primarily depends on rainfall, implying that higher levels of effective precipitation ensure greater water storage in the soil, which happens especially after the canopy closure.

Amazonas et al. (2018) examined water use in *Eucalyptus* monocultures and mixed stands and emphasized the importance of rainfall reaching the forest floor and the availability of water in the surface layers for fast-growing species (e.g., *Eucalyptus* spp.), particularly from the third year of growth until the end of the crop rotation. Although soil moisture was not monitored below a depth of 1.60 m in this study, the available data offer a reasonable interpretation of soil water use by the species investigated. We expected *E. camaldulensis* to exhibit higher soil moisture content, given its higher effective precipitation. As a more drought-resilient species, *E. camaldulensis* can access water from deeper soil layers during water deficit conditions. When more water is available, it allocates photoassimilates to develop both thick and fine roots in the topsoil to maximize water uptake (Doody et al., 2015). Compared to *E. grandis* and *E. urophylla, E. camaldulensis* has a higher specific root length and area, reflecting its greater capacity to explore the soil per unit of fine root biomass, as observed by Ávila (2020). This adaptive mechanism allows it to access water reserves more effectively. Germon et al. (2019) demonstrated that *Eucalyptus* can increase their specific root length and area by 15 % under water stress conditions, further supporting the role of this adaptation in enhancing water uptake.

5. Conclusions

This study provides compelling evidence that species selection based on WUE and transpiration dynamics is crucial for enhancing productivity while conserving water resources in Eucalyptus plantations. *E. urophylla* and *E. grandis* presented greater WUE. The findings suggest that *E. urophylla* is a particularly promising species for regions where both productivity and water use efficiency are critical considerations. In contrast, *E. camaldulensis* may be better suited to environments with more severe water limitations, where its drought-adaptive mechanisms can be fully utilized.

Importantly, this study reinforces the need for site-specific species selection, emphasizing that matching species traits with local environmental constraints is key to achieving sustainable forest production systems. Further research under more severe water deficit conditions is essential to fully characterize the physiological plasticity and long-term resilience of these species. Research in areas with a broader range of water availability is important to deepen our understanding of species-specific responses to varying soil and climatic conditions. This could enhance our ability to recommend suitable *Eucalyptus* species for different environmental conditions, optimizing both productivity and sustainability in forest plantations.

Funding

This study was partially funded by the Coordenação de Aperfeiçoamento de Pessoal de Nível Superior – Brasil (CAPES) – under Finance Code 001. The first author received a scholarship from CNPq (National Council for Scientific and Technological Development) to support part of this research. Additional financial support was provided by the Silviculture and Management Thematic Program at the Institute of Forest Research and Study (PTSM/IPEF). Open access funding was provided by the Swedish University of Agricultural Sciences (SLU).

CRediT authorship contribution statement

Amanda de Castro Segtowich: Writing – review & editing, Writing – original draft, Visualization, Validation, Supervision, Project administration, Methodology, Investigation, Formal analysis, Data curation. **Cassio Rafael Costa dos Santos:** Writing – review & editing, Writing – original draft, Visualization, Validation. **Maria Leidiane Reis Barreto:** Writing – review & editing, Writing – original draft, Visualization, Validation. **Nataly Foronda Ortega:** Writing – review & editing, Writing – original draft, Visualization, Validation. **Felipe Tavares Lima:** Writing – review & editing, Writing – original draft, Visualization, Validation. **Patrícia Andressa Ávila Franco de Carvalho:** Writing – review & editing, Visualization, Validation. **Juan Sinforiano Delgado Rojas:** Writing – review & editing, Visualization, Validation. **Alexandre de Vicente Ferraz:** Writing – review & editing, Validation, Supervision, Resources, Project administration, Methodology, Data curation, Conceptualization. **José Leonardo de Moraes Gonçalves:** Writing – review & editing, Validation, Supervision, Resources, Project administration, Methodology, Data curation, Conceptualization.

Declaration of competing interest

The authors declare that they have no known competing financial interests or personal relationships that could have appeared to influence the work reported in this paper.

Acknowledgments

We are grateful to CAPES/Brazil (grant number Code 001) and the National Council for Scientific and Technological Development – CNPq for providing the first author with an MSc scholarship during the development of this study. The authors also thank the Silviculture and Management Thematic Program at the Institute of Forest Research and Study (PTSM/IPEF) for their financial and technical support. We also thank the Forest Sciences Department of the University of São Paulo, "Luiz de Queiroz" College of Agriculture (ESALQ-USP), as well as the Experimental Station of Forest Sciences (EECF) in Itatinga, especially Rildo, Lourival, and Elaine, for their support during the fieldwork activities. We thank Dr. Juan Rojas for the technical and scientific support, as well as Dr. Joannès Guillemot for providing us with some equipment. To Eder and the Floragro team for their support in carrying out some fieldwork activities.

Data availability

The datasets generated during and/or analyzed during the current study are available from the corresponding author upon reasonable request.

References

Ávila, P.A., 2020. Aspectos Morfofisiológicos da Copa e do Sistema Radicular de Espécies de Eucalyptus e Corymbia Com Diferentes Tolerâncias à Deficiência Hídrica. University of São Paulo. Dissertation.

Abreu, M.C., Soares, A.A.V., Freitas, C.H., Martins, F.B., 2022. Transpiration and growth responses by *eucalyptus* species to progressive soil drying. J. For. Res. 33, 1529–1543. https://doi.org/10.1007/S11676-021-01448-Z/FIGURES/5.

Amazonas, N.T., Forrester, D.I., Oliveira, R.S., Brancalion, P.H.S., 2018. Combining *Eucalyptus* wood production with the recovery of native tree diversity in mixed plantings: implications for water use and availability. For. Ecol. Manage 418 (1), 34–40. https://doi.org/10.1016/J.FORECO.2017.12.006.

Avila-Diaz, A., Benezoli, V., Justino, F., Torres, R., Wilson, A., 2020. Assessing current and future trends of climate extremes across Brazil based on reanalyses and earth system model projections. Clim. Dyn. 55, 1403–1426. https://doi.org/10.1007/s00382-020-05333-z.

Baskerville, G.L., 1972. Use of logarithmic regression in the estimation of plant biomass. Canad. Jour. For. Res. 2 (1), 49–53. https://doi.org/10.1139/x72-009.

Barotto, A.J., Monteoliva, S., Gyenge, J., Martínez-Meier, A., Moreno, K., Tesón, N., Fernández, M.E., 2017. Wood density and anatomy of three *eucalyptus* species: implications for hydraulic conductivity. For. Syst. 26 (1), 1–11. https://doi.org/10.5424/fs/2017261-10446.

Bouvet, J.M., Makouanzi Ekomono, C.G., Brendel, O., Laclau, J.P., Bouillet, J.P., Epron, D., 2020. Selecting for water use efficiency, wood chemical traits and biomass with genomic selection in a *Eucalyptus* breeding program. For. Ecol. Manage 465, 118092. https://doi.org/10.1016/J.FORECO.2020.118092.

Câmara, A.P., Vidaurre, G.B., Oliveira, J.C.L., Toledo Picoli, E.A., Almeida, M.N.F., Roque, R.M., Tomazello Filho, M., Souza, H.J.P., Oliveira, T.R., Campoe, O.C., 2020.

Changes in hydraulic architecture across a water availability gradient for two contrasting commercial *Eucalyptus* clones. For. Ecol. Manage 474, 1–12. https://doi.org/10.1016/j.foreco.2020.118380.
Chen, X., Zhao, P., Ouyang, L., Zhu, L., Ni, G., Schäfer, K.V.R., 2020. Whole-plant water hydraulic integrity to predict drought-induced *eucalyptus* urophylla mortality under drought stress. For. Ecol. Manage 468, 1–10. https://doi.org/10.1016/J.FORECO.2020.118179.
Christina, M., Nouvellon, Y., Laclau, J.P., Stape, J.L., Bouillet, J.P., Lambais, G.R., Maire, G., 2017. Importance of deep water uptake in tropical eucalypt forest. Funct. Ecol. 31, 509–519. https://doi.org/10.1111/1365-2435.12727.
Climent, J., et al., 2024. Tradeofs and trait integration in tree phenotypes: consequences for the sustainable use of genetic resources. Cur. Fores. Rep. 10, 196–222. https://doi.org/10.1007/s40725-024-00217-5.
Crockford, R.H., Richardson, D.P., 2000. Partitioning of rainfall into throughfall, stemflow and interception: effect of forest type, ground cover and climate. Hydrol. Proc. 14, 2903–2920.
de Castro Segtowich, A., Langvall, O., Huuskonen, S., Fahlvik, N., Holmström, E., 2025. Swift adjustment of biomass allocation strategies in scots pine after thinning. Eur. J. For. Res. 144 (3), 699–714. https://doi.org/10.1007/s10342-025-01788-z.
Delgado-Rojas, J.S., 2008. Influência Da Adubação Em Plantação De *Eucalyptus Grandis* Sobre o Consumo De água Estimado Por Fluxo De Seiva. INRA, Paris, p. 30.
Delgado-Rojas, J.S., 2003. Avaliação Do Uso do Fluxo de Seiva e da Variação do Diâmetro do Caule e de Ramos na Determinação das Condições Hídricas de Citros. University of São Paulo como Base para o Manejo de Irrigação Thesis.
Doody, T.M., Colloff, M.J., Davies, M., Koul, V., Benyon, R.G., Nagler, P.L., 2015. Quantifying water requirements of riparian river red gum (*Eucalyptus camaldulensis*) in the Murray-Darling Basin, Australia - implications for the management of environmental flows. Ecohydrol 8. https://doi.org/10.1002/eco.1598.
Dubreuil, V., Fante, K.P., Planchon, O., Sant'Anna Neto, J.L., 2019. Climate change evidence in Brazil from Köppen's climate annual types frequency. Inter. Jour. Climat. 39, 1446–1456. https://doi.org/10.1002/joc.5893.
Dye, P., Vilakazi, P., Gush, M., Ndlela, R., Royappen, M., 2001. Investigation of the feasibility of using trunk growth increments to estimate water use of *eucalyptus grandis* and *Pinus patula* plantations. In: WRC Report 809/1/01. Pretoria, South Africa.
EMBRAPA, 2012. Sistema Brasileiro De Classificação De Solos. Centro Nacional de Pesquisa de Solos, Embrapa Solos, Rio de Janeiro, p. 353.
Engel, V., Jobbágy, E.G., Stieglitz, M., Williams, M., Jackson, R.B., 2005. Hydrological consequences of *Eucalyptus* afforestation in the Argentine Pampas. Water. Resour. Res. 41, 1–14. https://doi.org/10.1029/2004WR003761.
Ferraz, S.F.B., Rodrigues, C.B., Garcia, L.G., Alvares, C.A., Lima, W.P., 2019. Effects of *eucalyptus* plantations on streamflow in Brazil: moving beyond the water use debate. For. Ecol. Manage 453, 1–10. https://doi.org/10.1016/j.foreco.2019.117571.
Ferreto, D.O.C., Reichert, J.M., Lopes Cavalcante, R.B., Srinivasan, R., 2021. Rainfall partitioning in young clonal plantations *eucalyptus* species in a subtropical environment, and implications for water and forest management. Int. Soil and Wat. Conserv. Res. 9, 474–484. https://doi.org/10.1016/J.ISWCR.2021.01.002.
Florêncio, G.W.L., Martins, F.B., Fagundes, F.F.A., 2022. Climate change on *eucalyptus* plantations and adaptive measures for sustainable forestry development across Brazil. Ind. Crop. Prod. 188, 1–12. https://doi.org/10.1016/J.INDCROP.2022.115538.
Fonseca, S., Resende, M., Alfenas, A., Guimarães, L., Assis, T., Grattapaglia, D., 2010. Manual Prático de Melhoramento Genetico do Eucalipto. Editora UFV, Viçosa, p. 105.
Germon, A., Jourdan, C., Bordon, N., Robin, A., Nouvellon, Y., Chapuis-Lardy, L., Gonçalves, J.L.M., Pradier, C., Guerrini, I.A., Laclau, J.P., 2019. Consequences of clear-cutting and drought on fine root dynamics down to 17 m in coppice-managed eucalypt plantations. For. Ecol. Manage 445, 48–59. https://doi.org/10.1016/j.foreco.2019.05.010.
Gollan, T., Turner, N.C., Schulze, E.D., 1985. The responses of stomata and leaf gas exchange to vapour pressure deficits and soil water content - III. In the sclerophyllous woody species Nerium oleander. Oecol 65, 356–362. https://doi.org/10.1007/BF00378909/METRICS.
Gonçalves A.N., Mello, S.L.de M. (2015) O sistema radicular das árvores. Nutrição e fertilização florestal 427–il.
Gonçalves, J.L., Alvares, C.A., Rocha, H.T., Brandani, C.B., Hakamada, R., 2017. Eucalypt plantation management in regions with water stress. Sout. For.: Jour. For. Sci. 79 (3), 169–183. https://doi.org/10.2989/20702620.2016.1255415.
Gonçalves, J.L.M., Stape, J.L., Laclau, J.-P., Bouillet, J.-P., Ranger, J., 2009. Assessing the effects of early silvicultural management on long-term site productivity of fast-growing eucalypt plantations: the Brazilian experience. Sout. For.: Jour. For. Sci. 70, 105–118. https://doi.org/10.2989/SOUTH.FOR.2008.70.2.6.534.
Gonçalves, J.L .M, Alvares, C.A., Higa, A.R., Silva, L.D., Alfenas, A.C., Stahl, J., Ferraz, S. F.B., Lima, W.P., Brancalion, P.H.S., Hubner, A., Bouillet, J.P.D., Laclau, J.P., Nouvellon, Y., Epron, D., 2013. Integrating genetic and silvicultural strategies to minimize abiotic and biotic constraints in Brazilian eucalypt plantations. For. Ecol. Manage 301, 6–27. https://doi.org/10.1016/J.FORECO.2012.12.030.
Granier, A., 1985. Une nouvelle méthode pour la mesure du flux de sève brute dans le tronc des arbres. Ann. des Sci. For. 42, 193–200. https://doi.org/10.1051/forest:19850204.
Granier, A., Hue, R., Barigah, S.T., 1996. Transpiration of natural rain forest and its dependence on climatic factors. Agric. For. Meteorol. 78, 19–29. https://doi.org/10.1016/0168-1923(95)02252-X.
Hakamada, R., Hubbard, R.M., Ferraz, S., Stape, J.L., Lemos, C., 2017. Biomass production and potential water stress increase with planting density in four highly productive clonal *eucalyptus* genotypes. Sou. For. Jour. For. Sci. 79, 251–257. https://doi.org/10.2989/20702620.2016.1256041.
Herrera, A., Urich, R., Rengifo, E., Ballestrini, C., González, A., León, W., 2012. Transpiration in a eucalypt plantation and a savanna in Venezuela. Tr. Struct. Funct. 26, 1759–1769. https://doi.org/10.1007/S00468-012-0745-0/FIGURES/8.
Hubbard, R.M., Carneiro, R.L., Campoe, O., Alvares, C.A., Figura, M.A., Moreira, G.G., 2020. Contrasting water use of two *Eucalyptus* clones across a precipitation and temperature gradient in Brazil. For. Ecol. Manage 475, 1–9. https://doi.org/10.1016/j.foreco.2020.118407.
Kotowska, M.M., Link, R.M., Roll, A., Hertel, D., Holscher, D., Waite, P.-A., Moser, G., Tjoa, A., Leuschner, C., Schuldt, B., 2021. Effects of wood hydraulic properties on water use and productivity of tropical rainforest trees. Front. For. Gl. Chan. 3, 1–14. https://doi.org/10.3389/ffgc.2020.598759.
Lemcoff, J.H., Guarnaschelli, A.B., Garau, A.M., Prystupa, P., 2002. Elastic and osmotic adjustments in rooted cuttings of several clones of *Eucalyptus* camaldulensis Dehnh. From southeastern Australia after a drought. Fl: Morph. Distrib. Funct. Eco. Pl. 197, 134–142. https://doi.org/10.1078/0367-2530-00023.
Li, C., Li, B., Zhao, W., Jiang, J., Tang, J., 2025. Forest tree breeding under the global environmental change: challenges and opportunities. Trees. For. People 20, 1–11. https://doi.org/10.1016/j.tfp.2025.100867.
Lima W.P., Ferraz S.F.B., Rodrigues C.B., Voigtlaender M. (2012) Assessing the hydrological effects of forest plantations in Brazil. River conservation and management 59–68. https://doi.org/10.1002/9781119961819.CH5.
Lima, W.P., Jarvis, P., Rhizopoulou, S., 2003. Stomatal responses of *eucalyptus* species to elevated CO_2 concentration and drought stress. Sci. Agric. 60, 231–238. https://doi.org/10.1590/S0103-90162003000200005.
Lopes, B.A.B., Silva, A.M.M., Santana, M.C., Feiler, H.P., Pereira, A.P.A., Teixeira, M.F., Araújo, V.L.V.P., Ávila, P.A., Gonçalves, J.L.M., Staunton, S., 2022. Arbuscular mycorrhizal fungi and soil quality indicators in *eucalyptus* genotypes with different drought tolerance levels. Front. Fungal. Biol. 3, 1–13. https://doi.org/10.3389/ffunb.2022.913570, 913570.
Mariño Macana, Y.A., Corrêa, R.S., Toledo, F.H.S.F., Vicente Ferraz, A., Oliveira Ferreira, E.V., Hakamada, R.E., Moreira, G.G., Arthur Junior, J.C., Gonçalves, J.L.M., 2022. Soil fertility, root growth, and eucalypt productivity in response to lime and gypsum applications under soil water deficit. New. For. (Dordr) 54, 833–852. https://doi.org/10.1007/S11056-022-09943-9/FIGURES/6.
Martorell, S., Diaz-Espejo, A., Medrano, H., Ball, M.C., Choat, B., 2014. Rapid hydraulic recovery in *Eucalyptus pauciflora* after drought: linkages between stem hydraulics and leaf gas exchange. Plant Cell Environ. 37, 617–626. https://doi.org/10.1111/pce.12182.
Masullo, L.S., Derisso, V.D., Manarim, G.R., Ferraz, A.V., Rocha, J.H.T., Ávila, P.A., Florentino, A.L., Aguiar, C.L., Lavres, J., Gonçalves, J.L.M., 2022. Modulation of structural carbohydrates, phenol compounds and lignin content in *Eucalyptus urophylla* cuttings grown under boron, copper and zinc induced-deficiency. New. For. (Dordr) 53, 337–352. https://doi.org/10.1007/S11056-021-09859-W/FIGURES/2.
Melo Neto, J.O., Rodrigues, A.F., Mello, C.R, 2024. On canopy rainfall interception modeling in a *eucalyptus* plantation. For 15 (1577), 1–15. https://doi.org/10.3390/f15091577.
Mielke, M.S., Oliva, M.A., Barros, N.F., Penchel, R.M., Martinez, C.A., Fonseca, S., Almeida, A.C., 2000. Leaf gas exchange in a clonal eucalypt plantation as related to soil moisture, leaf water potential and microclimate variables. Tr. Struc. Func. 14, 263–270. https://doi.org/10.1007/S004680050012/METRICS.
Paula, R.C., Paula, N.F., Marino, C.L., 2011. Melhoramento De Espécies Perenes Para Condições De Estresses abióticos. Melhoramento de Plantas Para Condições De Estresses abióticos. Suprema. Visconde de Rio Branco, p. 50.
Quiñones Martorello, A.S., Gyenge, J.E., Colabelli, M.N., Petigrosso, L.R., Fernández, M. E., 2023. Functional responses to multiple sequential abiotic stress (waterlogging-drought) in three woody taxa with different root systems and stress tolerance. Physiol. Plant 175, 1–12. https://doi.org/10.1111/PPL.13958.
R Core Team, 2022. R: A language and Environment For Statistical Computing. R Foundation for Statistical Computing, Vienna. https://www.R-project.org [accessed on 28.05.2023].
Rocha, J.H.T., Goncalves, J.L.M., Ferraz, A.V., Poiati, D.A., Junior, J.C.A., Hubner, A., 2019. Growth dynamics and productivity of an *Eucalyptus grandis* plantation under omission of N, P, K Ca and Mg over two crop rotation. For. Ecol. Manage 447, 158–168. https://doi.org/10.1016/j.foreco.2019.05.06.
Saadaoui, E., Ben Yahia, K., Dhahri, S., Ben Jamaa, M.L., Khouja, M.L., 2017. An overview of adaptative responses to drought stress in *Eucalyptus spp*. For. Stud. 67, 86–96. https://doi.org/10.1515/fsmu-2017-0014.
Santos, B.M., Balbuena, T.S., 2017. Carbon assimilation in *Eucalyptus urophylla* grown under high atmospheric CO2 concentrations: a proteomics perspective. J. Proteomics. 150, 252–257. https://doi.org/10.1016/J.JPROT.2016.09.010.
Sivananthawerl, T., Mitlohner, R., 2003. Plant water relations as indicators for eucalyptus spp. Selection for new planting sites in Nuwaraeliya division of Sri Lanka. Cey. J. Sci. (Bio. Sci.) 31, 1–11.
Stape, J.L., Binkley, D., Ryan, M.G., Gomes, A.D.N., 2004. Water use, water limitation, and water use efficiency in a Eucalyptus plantation. Rev. Bosq. 25, 35–41.
Steenhuis, T.S., Alemie, T.C., Muche, H., Tilahun, S.A., Zimale, F.A., Mhiret, D.A., 2023. Effect of *Eucalyptus* on blue and green water availability and discharge in the tropical highlands: an interpretation of available literature. Jour. Hydrol. Hydromec. 71, 221–230. https://doi.org/10.2478/johh-2023-0020.
Virtuoso, M.C.S., Souza, J.V.O., Zanatto, B., Valente, T.S., Silva, E.H.C., Paula, R.C., 2022. Germinative and physiological performance of *eucalyptus* species under abiotic stress. Tr. For. Peop. 10, 1–8. https://doi.org/10.1016/j.tfp.2022.100348.

White, D.A., Turner, N.C., Galbraith, J.H., 2000. Leaf water relations and stomatal behavior of four allopatric *eucalyptus* species planted in Mediterranean southwestern Australia. Tr. Physiol. 20, 1157–1165. https://doi.org/10.1093/treephys/20.17.1157.

Whitehead, D., Beadle, C.L., 2004. Physiological regulation of productivity and water use in *Eucalyptus:* a review. For. Ecol. Manage 193, 113–140. https://doi.org/10.1016/J.FORECO.2004.01.026.

Yang, Y.J., Tong, Y.G., Yu, G.Y., Zhang, S.B., Huang, W., 2018. Photosynthetic characteristics explain the high growth rate for *eucalyptus camaldulensis*: implications for breeding strategy. Ind. Crops. Prod. 124, 186–191. https://doi.org/10.1016/J.INDCROP.2018.07.071.

Yousaf, M.S., Hassan Farooq, T., Ahmad, I., Mohsin Gilani, M., Haroon Rashid, M.U., Prasad Gautam, N., Islam, W., Asif, M., Wu, P., 2018. Effect of drought stress on the growth and morphological traits of *eucalyptus camaldulensis* and eucalyptus citriodora. PSM Biol. Res. 3, 85–91.

Zhang, H., Zhao, Y., Zhu, J.K., 2020. Thriving under stress: how plants balance growth and the stress response. Dev. Cell 55, 529–543. https://doi.org/10.1016/j.devcel.2020.10.012.

Zhang, Z., Zhao, P., McCarthy, H.R., Ouyang, L., Niu, J., Zhu, L., Ni, G., Huang, Y., 2016. Hydraulic balance of a *eucalyptus urophylla* plantation in response to periodic drought in low subtropical China. Front. Plant Sci. 7, 1–12. https://doi.org/10.3389/fpls.2016.01346.

Zhang, J., Han, D., Song, Y., Dai, Q., 2018. Study on the effect of rainfall spatial variability on runoff modeling. Jour. Hydroinfo. 20 (3), 577–587.